Atmos. Meas. Tech., 15, 4307–4322, 2022
https://doi.org/10.5194/amt-15-4307-2022

Atmospheric Measurement Techniques
Open Access
EGU

Impact of the revisit frequency on cloud climatology for CALIPSO, EarthCARE, Aeolus, and ICESat-2 satellite lidar missions

Andrzej Z. Kotarba

Space Research Centre, Polish Academy of Sciences, 00-716 Warsaw, Poland

Correspondence: Andrzej Z. Kotarba (akotarba@cbk.waw.pl)

Received: 9 March 2022 – Discussion started: 11 March 2022
Revised: 20 June 2022 – Accepted: 21 June 2022 – Published: 28 July 2022

Abstract. Space profiling lidars offer a unique insight into cloud properties in Earth's atmosphere and are considered the most reliable source of total (column-integrated) cloud amount (CA), and true (geometrical) cloud top height (CTH). However, lidar-based cloud climatologies suffer from infrequent sampling: every n days, and only along the ground track. This study therefore evaluated four lidar missions, namely CALIPSO (revisit every $n = 16$ d), EarthCARE ($n = 25$), Aeolus ($n = 7$), and ICESat-2 ($n = 91$), to test the hypothesis that each mission provides accurate data on CA and CTH. CA/CTH values for a hypothetical daily revisit mission were used as reference (data simulated with Meteosat 15 min cloud observations, assumed to be a proxy for ground truth). Our results demonstrated that this hypothesis is invalid, unless individual lidar transects are averaged over an area $10 \times 10°$ in longitude and latitude (or larger). If this is not the case, the required accuracy of 1 % (for CA) or 150 m (for CTH) cannot be met, either for a single-year annual or monthly mean, or for a > 10 year climatology. A CALIPSO-focused test demonstrated that the annual mean CA estimate is very sensitive to infrequent sampling, and that this factor alone can result in 14 % or 7 % average uncertainty with 1 or 2.5° resolution data, respectively. Consequently, applications that use gridded lidar data should consider calculating confidence intervals, or a similar measure of uncertainty. Our results suggest that CALIPSO, and its follow-on mission EarthCARE, are very likely to produce consistent cloud records despite the difference in sampling frequency.

1 Introduction

Accurate knowledge of cloud properties is essential for reliable modelling of the atmosphere, including climate processes (Stephens, 2005; Trenberth et al., 2009). Among the many techniques used to assess cloud presence and parametrization, satellite remote sensing plays an essential role (Stephens and Kummerow, 2007). However, like other climate datasets, satellite-based climatologies face limitations related to spatial and/or temporal sampling regimes.

The coverage and frequency of satellite observations are determined primarily by the satellite's orbit, and then by the design of the cloud-sensing instrument. For a typical atmospheric mission, daily global coverage is obtained with a platform that operates from a sun-synchronous orbit: namely, a near-circular path, which is inclined at $\sim 98°$ to the equatorial plane, at an altitude of up to 1000 km above Earth's surface (Capderou, 2005). A sun-synchronous orbit can be designed in such a way that the satellite's ground-track repeats precisely every n days: in other words, every n days a satellite will pass over the same location, and observe the land, ocean, or atmosphere under exactly the same viewing geometry as n days before. The length of the revisit period (expressed in days, or number of revolutions) is constant for a mission, but may differ between missions, depending on the scientific goal (Table 1).

A less-frequent revisit schedule produces a denser ground track pattern, as the distance between adjacent tracks becomes shorter. If a sensor's cross-track field of view (FOV) is larger than the distance between ground tracks at the Equator, a single polar-orbiting mission has the ability to collect data for every single location on Earth, daily. However, when the FOV is narrower, the situation becomes challenging. Extremely narrow FOVs are specific to cloud profiling lidar sen-

Table 1. Ground track layout parameters for the sun-synchronous lidar missions investigated in our study. EQT refers to the equatorial crossing time for the ascending node, and is given in mean local solar time (LST). The full names of the lidar instruments are: the Advanced Topographic Laser Altimeter System (ATLAS), the Cloud-aerosol Lidar with Orthogonal Polarization (CALIOP), the Atmospheric Lidar (ATLID), the Atmospheric Laser Doppler Instrument (ALADIN).

Mission name	Lidar instrument	Ground track repeated every		Ground tracks separation		EQT (LST)	Inclination deg.
		n days	orbits	km	deg.		
Aeolus	ALADIN	7	111	360.6	3.24	18:00	97.0
CALIPSO	CALIOP	16	233	171.8	1.55	13:30	98.2
EarthCARE	ATLID	25	389	102.9	0.93	14:00	97.1
ICESat-2	ATLAS	91	1387	28.8	0.26	–	92.0

sors. Unlike imagers, profiling instruments do not focus on the spatial distribution of clouds, but on their vertical structure. To obtain vertically-resolved information, lidars emit pulses almost directly towards the nadir. The resulting swath is less than 1 km wide, therefore obtaining global coverage is technically impossible: most locations are never sampled, while others are probed only once every n days (twice if ascending and descending parts of an orbit intersect).

Despite this narrow FOV, lidars are of great importance for cloud climatology. These active instruments operate very efficiently during both day and night, unlike imagers that tend to underestimate night-time cloud amount, or fail to provide cloud optical properties when no solar illumination is available (Vaughan et al., 2009; Liu et al., 2010). Moreover, lidars can detect atmospheric features based on the time delay of the backscattered signal, which makes a direct calculation of cloud top geometrical height possible (Holz et al., 2009). Vertically resolved information from lidars helps to unambiguously discriminate clouds and aerosols from the background, especially for locations where the spectral and/or thermal contrast between cloud and the background is low (Liu et al., 2009). Finally, lidars are much more sensitive to optically-thin clouds than imagers, therefore lidar-based climatologies of cirrus, or column-integrated total cloud amount datasets are considered to be the most reliable (Mace and Zhang, 2014; Nazaryan et al., 2008).

The main source of lidar-based cloud data is the Cloud-Aerosol Lidar and Infrared Pathfinder Satellite Observation (CALIPSO) mission, equipped with the Cloud-Aerosol Lidar with Orthogonal Polarization (CALIOP; Winker et al., 2003). Launched in 2006, CALIPSO has been profiling the atmosphere with a revisit cycle of $n = 16$ d (233 orbits; Table 1). At the time of writing (the beginning of 2022), the mission has already been extended, and is approaching the end of its lifetime. It will be followed by the EarthCARE mission ($n = 25$ d), which will launch no earlier than 2023 (Illingworth et al., 2015). Two other lidar satellites that have operated in space simultaneously with CALIOP are Aeolus (Stoffelen et al., 2005), and ICESat-2 (Markus et al., 2017). The former features a Doppler wind lidar, while the latter focuses on ice altimetry and vegetation. Both missions are capable of providing limited information on clouds, but are not optimized for that goal (Flamant et al., 2008; Palm et al., 2021).

Lidars have also been deployed on non-sun-synchronous orbits. Examples include the Cloud-Aerosol Transport System (CATS; active between 2015–2017; Yorks et al., 2016), the Global Ecosystem Dynamics Investigation (GEDI; active since 2018; Tang et al., 2019), or the Multi-footprint Observation Lidar and Imager (MOLI; planned for 2022; Daisuke et al., 2020), which have all been designed as host payloads for the International Space Station. The inclination of the Station's orbit restricts observations to latitudes between 51.6° N and 51.6° S, while its non-synchronous nature makes it possible to detect diurnal cloud cycles (Noel et al., 2018) – which cannot be achieved by polar-orbiting lidar missions that operate along a fixed ground track.

Lidar profiles from CALIPSO and other missions are explored in their native geometry (swath data, Level 2); however climate-oriented applications frequently use gridded (Level 3) global datasets (Chepfer et al., 2010). When gridded, individual transects are aggregated into mean monthly, seasonal, or annual values, and averaged over predefined grid boxes. Practical considerations mean that the grid resolution should correspond to the separation between adjacent ground tracks at the Equator, resulting in a gap-free global map. For instance, the separation for CALIPSO is 1.55° (or 172 km; Table 1); therefore, global gridded datasets from the mission are usually generated at 2° resolution or coarser (e.g. Chepfer et al., 2010; Ma et al., 2013; Kodama et al., 2012).

In gridded form, lidar observations serve primarily as ground truth for validating atmospheric models (e.g. Chepfer et al., 2008; Kodama et al., 2012; Konsta et al., 2016), or cloud climatologies from other sensors (e.g. Wylie et al., 2007; Boudala and Milbrandt, 2021; Ackerman et al., 2008; Liu et al., 2010), and they can also be analysed as independent, stand-alone cloud climatologies (e.g. Mace et al., 2009; Adhikari et al., 2012; Oreopoulos et al., 2017). Applications that rely on gridded data can accommodate the sparse and infrequent lidar sampling regime. Specifically, it is routinely assumed that an n day revisit schedule is sufficient to provide an accurate and reliable estimate of cloud parameters for a

predefined location (grid box), and time frame (monthly to annual average). However, this assumption has never been validated.

Lidar sampling schemes become even more significant when data from an n day revisit are compared to cloud climatologies originating from imagers with an effective 1 d schedule. In the absence of a detailed analysis, it is impossible to identify which of the differences between datasets can be explained by inconsistent sampling schemes. Past studies (e.g. Liu et al., 2012; Kotarba and Solecki, 2021) have demonstrated that the sample size of lidar (or radar) transects impacts the uncertainty range for mean cloud amount, and appropriate confidence intervals have been suggested. Nevertheless, these studies have not addressed the key question: how closely does n day-revisit data actually approximate a 1 d revisit (imager-like) climatology? This question motivated the present study.

Therefore, this study investigates the hypothesis that cloud parameters estimated from an n day revisit mission do not differ significantly from values that would be obtained with a daily revisit. The hypothesis is tested for monthly/annual means of cloud amount (CA), and cloud top height (CTH), explored over a wide range of grid resolutions (1–10° latitude/longitude). Since there are no lidar missions with a 1 d revisit schedule, the necessary data were simulated with high-temporal-resolution observations from the Meteosat satellites. Special attention is paid to CALIOP, and other sun-synchronous lidar missions are also considered for reference.

2 Data and methods

Sun-synchronous missions always cross the Equator at the same local solar time (LST), while the latter corresponds to a different Universal Time Coordinated (UTC) hour for each transect. In order to simulate a 1 d revisit as closely as possible, lidar ground tracks must be linked with appropriate (in terms of UTC) cloud observations. Additionally, it is important that the source of cloud data is the same for all missions of interest, thus, observations must be recorded at a high temporal cadence. This requirement was met by the Meteosat satellites.

The Meteosat series are in geostationary orbit (0° E). Each satellite is equipped with the Spinning Enhanced Visible and InfraRed Imager (SEVIRI), that scans Earth's disc every 15 min at 1 km per pixel spatial resolution at nadir. SEVIRI's radiances are processed into a number of geophysical products. This study uses the CLoud property dAtAset using SEVIRI (CLAAS, version 2; Stengel et al., 2014; Benas et al., 2017; Finkensieper et al., 2020). All CLAAS data files were accessed from the EUMETSAT Satellite Application Facility on Climate Monitoring (CM SAF).

Two parameters were investigated: cloud amount (CA; expressed on a 0 %–100 % scale), calculated from the CLAAS Cloud Mask product; and cloud top height (CTH; in metres), based on the Cloud Top Properties product. These parameters were chosen as they are the most accurately reported by space lidars (Winker et al., 2017). Although lidars also provide high-quality estimations of cloud optical thickness (COT), the latter parameter was not included in the study, since Meteosat is not able to estimate it at night (unlike lidars). CA and CTH are available both day and night, both from lidars and imagers.

In this study, although Meteosat observations are considered as reference, they should not be interpreted as ground truth for CA/CTH. Like other missions, Meteosat has limitations regarding both cloud detection and parametrization. For instance, Benas et al. (2017) found that the probability of cloud detection with the CLAAS scheme was 87.5 % (for all clouds), or 96.2 % (for clouds of optical thickness greater than 0.2) compared to CALIPSO detections. The same study revealed CLASS cloud top properties (including CTH) to be highly correlated with CALIPSO estimates (Pearson's coefficient between 0.84 and 0.88), while Stengel et al. (2014) noted that CLASS underestimated CTH by 0.7 km.

It should therefore be noted that the reason for using Meteosat in this study was not to provide absolute values of CA/CTH, but rather to create a time series of very realistic representations of CA/CTH at high spatial and temporal resolution.

The simulation considered the following sun-synchronous lidar missions:

- The CALIPSO mission was launched in 2006, and it is the most important source of lidar-based, long-term cloud data. The satellite, which is designed for cloud and aerosol studies, operates at two wavelengths (532 and 1064 nm), with an along track laser pointing 3° off-nadir (initially 0.3°; Hunt et al., 2009). Between 2006 and 2018, the satellite flew in formation with other satellites in NASA's A-Train Constellation, contributing a unique dataset of multi-sensor collocated measurements. It remains operational, in a drifting orbit (Braun et al., 2019). CALIPSO is included in this study to gain an insight into the reliability of its cloud climatology, in a context of sparse sampling and infrequent revisits.

- The EarthCARE mission is currently (January 2022) expected to launch in 2023. This CALIPSO follow-on mission will, like CALIPSO, use an afternoon orbit (equatorial crossing time 14:00 LST, ascending node), but follow a less-frequent revisit schedule ($n = 25$ d). EarthCARE's along track lidar is expected to point 3° off-nadir, and operate in the ultraviolet domain at 355 nm (Illingworth et al., 2015). EarthCARE is included in the present study to provide a general insight into CALIPSO data integrity, in terms of the revisit cycle.

– The Aeolus mission launched in 2018, and is designed to measure wind profiles with an ultraviolet (355 nm) Doppler lidar. The satellite is in an polar orbit with a crossing time at 18:00 LST (ascending node; dawn–dusk orbit). To meet mission requirements, Aeolus' across-track laser points 35° off-nadir, meaning that a measurement track is located 230 km parallel to the ground track (Stoffelen et al., 2005). The present study, however, approximates that the lidar operates in nadir geometry. Aeolus is included for reference, as an example of a mission with a frequent revisit schedule ($n = 7$ d).

– The ICESat-2 mission launched in 2018; the goal is to provide accurate laser altimetry for cryosphere and vegetation. The mission is characterized by a long revisit cycle ($n = 91$ d), resulting in a dense ground track: path separation at the Equator is only 29 km. ICESat-2's altimeter operates in the visible domain (532 nm), its six laser beams are grouped in three pairs, separated by ~ 3.3 km. The actual pointing scheme changes between the polar regions and lower latitudes (see Markus et al., 2017, for details). In the present study, the configuration is simplified to one beam coinciding with nadir. ICESat-2 is included for reference, as an example of a mission with a very infrequent revisit regime.

For each mission, the simulation procedure was as follows.

1. The ground track was generated based on orbital parameters, accessed in the form of Two-Line Elements (TLE). The ground track covered the full revisit cycle (of n days), and provided geographical coordinates of sub-satellite points every one second. TLE for CALIPSO, Aeolus, and ICESat-2 were obtained from an online archive (https://celestrak.com/, last access: 21 June 2022). Elements for EarthCARE (yet to be launched) were kindly provided by Rob Koopman and Montserrat Pinol Solé of the European Space Agency. Although EarthCARE TLE are fully representative of the final configuration, there is still one degree of freedom that will be defined post-launch (namely, the final choice of the longitude of the ascending node crossing at the Equator), but this had no impact on the results of the present study.

2. Each ascending and descending fragment of each orbit in a revisit cycle was individually projected onto the Meteosat native coordinate system: namely, a vertical perspective from a geostationary orbit over 0° E.

3. Every pixel in the Meteosat-projected transect was assigned cloud amount (CA), and cloud top height (CTH) data from the collocated Meteosat product. The assignment always used the Meteosat observation that was closest in time to the lidar's pass, taking the lidar's UTC time of the ascending or descending node as reference. The procedure was repeated for every day in a year; consequently, each ascending/descending transect was characterized by 365 (366) CA/CTH values annually. A total of 10 years of Meteosat data were used for the simulation (2007–2016), corresponding to 40 full cycles of ICESat-2 data, 146 of EarthCARE, 228 of CALIPSO, and 521 of Aeolus. Importantly, only one Meteosat observation per day and per mission was considered, meaning that the resulting climatologies represent the state of the atmosphere during a lidar overpass (i.e. they are biased to the local solar time and resemble real, lidar-based climatologies).

4. Simulated transects were then gridded into regular latitude-longitude grids of 1, 2.5, 5, and 10°. These various resolutions were considered in order to evaluate how differences between n day and 1 d climatology relate to the spatial aggregation scheme.

5. Finally, gridded transects were averaged into monthly and annual CA/CTH values. At this stage, data were filtered in two ways: (1) the selection of transects that reflected the n day revisit scheme; and (2) the selection of all data for all days (i.e. simulating a daily revisit).

The resulting (simulated) cloud climatology consisted of 120 monthly means, and 10 annual means, for two parameters (CA, CTH), four satellites (CALIPSO, EarthCARE, Aeolus, ICESat-2), four grid resolutions, and two sampling scenarios (1 d, n day). It is important to note that no actual cloud data from the lidar missions were used. The only real information exploited was the mission-specific ground track layout (orbital parameters). Actual CA/CTH observations were replaced by Meteosat data, in order to simulate a daily revisit. Since all lidar data were simulated, and all data originated from Meteosat, the only differences between missions were due to different orbital configurations: namely, ground track density, revisit frequency, and equatorial crossing time.

In order to eliminate Meteosat data collected under the most unfavourable geometry (the edge of Earth's disc, where the Meteosat line of sight is tangent to the sphere), only Meteosat locations within ±70° longitude and latitude were considered. Consequently, the study does not cover polar regions, where the ground track of polar-orbiting satellites is densest.

Statistical analyses focused on differences between the n day and the 1 d climatology (mean difference, and mean absolute difference). One-day means were always subtracted from n day values: a positive difference indicates that n day observations overestimated the CA/CTH value, whereas a negative difference represents the opposite case. If our hypothesis is valid, differences should be close to, or equal to zero. Whenever the terms "accuracy", or "error" are used, they refer to Meteosat 1 d estimates, which are assumed to be ground truth for the purposes of this study.

3 Results

3.1 Differences between a 1 d and an *n* d revisit regime

The analysis found that mean global differences between 1 d (simulated-hypothetical) and *n* day (simulated-actual) cloud climatologies were insignificant. Specifically, they never exceeded 0.1 % for CA, and 10 m for CTH – regardless of the satellite mission, spatial resolution of the final grid, or timeframe of averaged data (monthly or annual).

However, the data aggregation approach did find differences between 1 d and *n* day datasets when they were interpreted in terms of absolute values. Here, the magnitude of discrepancies was largest at the finest resolution, and decreased as the grid box size increased. Regarding monthly means (Table 2), there was a decrease from ~ 11 % at 1° to ~ 2 % at 10° for CA, and from ~ 1500 m at 1° to ~ 300 m at 10° for CTH. The same trend was observed for annual means, except that the absolute difference was 3–4 times lower compared to monthly values.

At 1° resolution, Aeolus performed slightly better than the other missions. In this case, monthly mean *n* day and 1 d estimates differed (on average) by 8.6 % (CA), and 1150 m (CTH). Corresponding discrepancies for other the lidar missions were in the range 11 %–12 %, and 1562–1686 m. However, as the resolution fell to 2.5° (or lower), discrepancies noted for Aeolus reached levels observed for CALIPSO and EarthCARE. On the other hand, ICESat observations appeared to be least accurate – but only at 1 and 2.5° – where the mission reported slightly higher discrepancies than EarthCARE or CALIPSO. At coarser resolutions, statistics were in close agreement for all four missions for 1 d and *n* day climatologies.

A more detailed overview of the actual agreement between mission scenarios was revealed by the distributions of differences. Negligibly small differences in CA and CTH for global means (Table 2) suggested no bias in the data, and Fig. 1 highlights that they were only an effect of error balancing. Infrequent sampling (every *n* days) led to a CA overestimation of 2 %–4 %, and a CTH underestimation of 100–200 m, according to the location of the peak frequency in distributions.

The highest monthly differences exceeded ± 30 % (CA), and ± 2 km (CTH) at 1° resolution. As expected, the spread of the differences (shape of the distribution) was a function of the observation aggregation strategy. Distributions were asymmetric at 1° resolution, and became more Gaussian for larger grid box sizes. The normalization of distributions was especially evident for monthly means (Fig. 1a–f), while annual means were always symmetric and close to normal (Fig. 1g–l).

A decrease in spatial resolution also resulted in the convergence of distributions. At 5°, the frequency of differences in CA/CTH was almost identical (Fig. 1c, f, i, and l), both for monthly and annual means. At such a high level of spatial generalization, the actual revisit time of a profiling lidar ($n = 7$, 16, 25, or 91 d) had no significant impact on CA/CTH estimations.

The distribution of differences in CA/CTH for annual means confirmed the (dis)similarities between missions already noted for globally-averaged data. Interestingly, two missions (namely CALIPSO and EarthCARE) shared nearly exactly the same distribution. Despite their different revisit frequencies (16 and 25 d), both missions reproduced the 1 d cloud climatology with the same accuracy, both for monthly and annual timescales, and regardless of the spatial resolution of the target global grid.

Geographical regions where discrepancies in CA/CTH between *n* day and 1 d climatologies were smallest are highlighted in Fig. 2. Regarding CA, the best agreement was noted for oceans at high latitudes ($> 45°$ N and $> 45°$ S), where the mean absolute difference between datasets typically did not exceed ~ 5 % on the monthly time scale. Lower latitudes featured absolute differences ranging between 5 % and 10 %, with only local exceptions of 10 %–15 % (e.g. Spain, northern Argentina, small parts of the east coast of Africa). Absolute errors in CTH estimations were largest over North Africa (the eastern Sahara Desert), exceeding ~ 1.5 km. On the other hand, the best agreement in CTH was found for the eastern Atlantic, at 0–30° N (a region of frequent marine stratocumulus), where CTH were reported to ± 0.5 km accuracy, or better.

The geographical distribution of absolute differences in CA/CTH estimations was controlled by two major relationships. First, the magnitude of differences depended on average CA for a location. In very cloudy, or almost cloudless regions, discrepancies in CA estimations were smallest (Fig. 3a), since their presence could be probed with the same efficiency, regardless of the revisit schedule. On the other hand, differences in CTH tended to decrease as CA increased, over the full range of cloudiness (Fig. 3e). The second relationship linked the discrepancy in a parameter estimation with the number of observations. As expected, the more frequently a grid box was sampled by a lidar, the lower the absolute difference between *n* day and 1 d climatologies both for CA (Fig. 3c), and CTH (Fig. 3g).

Since both average CA (Fig. 3d), and the number of observations (Fig. 3h) depended on latitude, the related parameters (CA, CTH) showed a similar dependency (Fig. 3b and f) modulated at the region level by CA (and the underlying global-scale circulation patterns). Specifically, the 1 d climatology was most accurately reproduced by *n* day data at high latitudes (high CA and frequent revisits are consistent with smaller differences), but with lower accuracy at lower latitudes (higher differences are due to less frequent revisits, regionally modulated by variable CA). This spatial pattern was

Table 2. Difference in mean global cloud amount (CA), and cloud top height (CTH) between a hypothetical 1 d revisit mission, and the actual n day revisit. Single-year monthly and annual means for 2005–2016 are considered.

	Differences in monthly means						Differences in annual means					
Lidar	CA (%)			CTH (m)			CA (%)			CTH (m)		
mission	diff	std	|diff|	diff	std	|diff|	diff	std	|diff|	diff	std	|diff|
	$1 \times 1^\circ$ grid box size											
Aeolus	0.01	11.2	8.6	4	1544	1150	0.02	3.2	2.5	−1	435	331
CALIPSO	0.04	15.3	11.6	6	2071	1562	0.04	4.3	3.3	6	610	458
EarthCARE	−0.02	15.0	11.5	−3	2091	1582	−0.01	4.2	3.3	1	605	460
ICESat	0.01	16.0	12.3	−10	2212	1686	0.02	4.4	3.5	−1	643	490
	$2.5 \times 2.5^\circ$ grid box size											
Aeolus	0.01	7.7	5.9	−2	1092	810	0.01	2.2	1.7	−2	302	232
CALIPSO	0.03	7.8	6.0	7	1145	860	0.03	2.2	1.7	5	315	245
EarthCARE	−0.02	7.7	5.9	2	1131	848	−0.01	2.2	1.7	< 1	313	242
ICESat	0.02	8.4	6.5	−3	1257	935	0.02	2.4	1.9	−3	347	267
	$5 \times 5^\circ$ grid box size											
Aeolus	0.01	4.8	3.7	−4	676	506	0.01	1.4	1.0	−3	188	145
CALIPSO	0.04	4.7	3.6	6	688	520	0.04	1.3	1.1	5	191	149
EarthCARE	< 0.01	4.6	3.5	1	674	509	< 0.01	1.3	1.0	< 1	187	146
ICESat	0.03	4.6	3.6	< 1	716	534	0.03	1.3	1.0	−3	169	152
	$10 \times 10^\circ$ grid box size											
Aeolus	0.02	2.7	2.1	−6	370	281	0.02	0.7	0.6	−5	105	82
CALIPSO	0.04	2.6	2.0	4	381	292	0.04	0.7	0.6	4	106	83
EarthCARE	−0.02	2.5	1.9	−1	360	279	−0.02	0.7	0.5	−1	99	77
ICESat	0.03	2.8	2.1	< 1	429	325	0.03	0.7	0.6	−2	117	91

observed across all investigated missions, both for monthly (Fig. 2, left panel), and annual means (Fig. 2, right panel). This variance in the magnitude of differences between missions, resolutions and timescales reflects trends observed for cloud distribution (Fig. 1).

3.2 Exploring an alternative revisit frequency for a CALIPSO-like mission

The results presented so far relate to satellite missions with a specific orbital configuration: namely, a fixed revisit frequency (every n days), and a native ground track layout. For instance, in the case of CALIPSO, differences in CA and CTH were calculated for 1 and 16 d climatologies, evaluated as spatial and temporal aggregations of instantaneous observations. However, another interesting question is how the selection of an n value itself impacts differences in CA/CTH. This question was answered with a test focused on the CALIPSO mission alone.

Simulation runs for CALIPSO assuming $n = 1$ (a reference, high temporal resolution climatology) and $n = 16$ (the actual revisit frequency) were supplemented with an additional 14 runs for all n between 1 and 16. Next, CA and CTH values for the 1 d revisit were subtracted from each n day revisit estimate. The resulting statistics are summarized in Fig. 4. This figure shows that absolute differences in both CA and CTH increased as the revisit period increased. Importantly, the change was gradual, with no rapid variation in discrepancies. Regarding the impact of spatial resolution, a general rule was that doubling the grid box size reduced the range of differences by half for all n.

At the finest spatial resolution (1°) the spread of differences in CA was so large that even a 2 d revisit would not be enough to keep them within a ±1 % range. However, CALIPSO observations are most frequently gridded at 2.5° resolution. In this case, a constellation of six CALIPSO-like observatories at adequately phased orbits would be sufficient to provide ±1 % accuracy for ∼ 80 % of locations (grid boxes) in the study area. It should be noted, however, that a 2 d revisit (equivalent to eight satellites) would be necessary to achieve 1 % accuracy in CA for all locations. Similar tendencies were observed for CTH at 2.5°. To obtain CTH statistics that differ from a 1 d climatology by no more than ±150 m, a constellation of eight CALIPSO-like missions would be required (equivalent to a 2 d revisit). A 3 d revisit schedule resulted in ±150 m accuracy for 80 % of locations in the study area. At coarser resolutions (5–10°) there

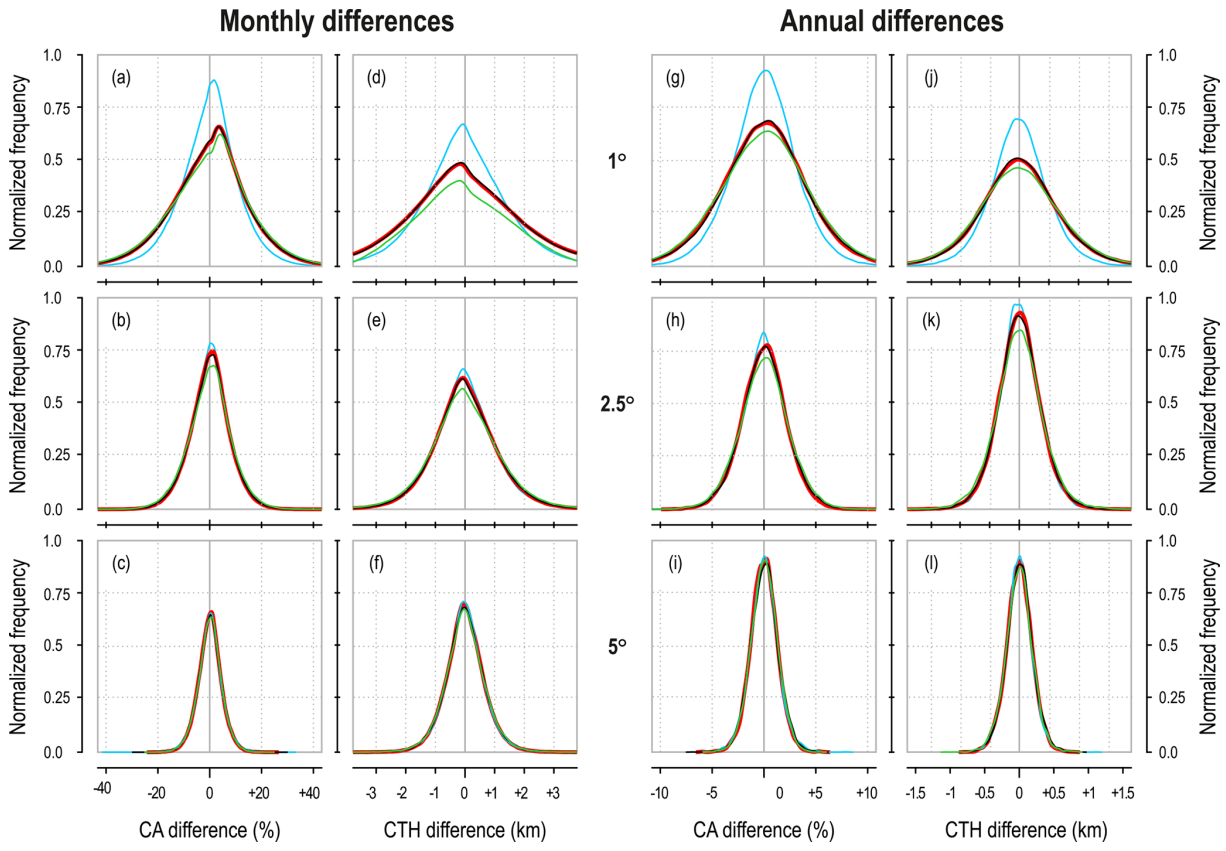

Figure 1. Differences between n day and 1 d revisit cloud amounts, and cloud top heights at monthly **(a–f)**, and annual **(g–l)** mean timescales, for CALIPSO (red), EarthCARE (black), Aeolus (blue), and ICESat-2 (green). In all cases, n day values are subtracted from 1 d values.

was no substantial decrease in CTH accuracy (with respect to a 1 d revisit) when n was 6 d or more. On the other hand, it should be noted that CALIPSO data gridded at $\leq 5°$ are only used occasionally.

3.3 Offset of the initial day of a revisit cycle

The revisit cycle of any mission in a sun-synchronous orbit is "anchored" to the satellite's launch date. For instance, CALIPSO started its 233-orbit cycle on 28 April 2006 – the day the satellite was deployed. Consequently, the annual mean of a cloud property reported by CALIPSO relies on data observed at a specific time and location, defined by a ground track that was initiated on that day (and repeated every 16 d ever since).

When deriving a cloud climatology, it is assumed that the temporal offset related to the start day of a revisit cycle should have no impact on the annual mean of a cloud parameter. That may be true for wide-swath imagers, but is questionable for profiling lidars, when the annual mean is based on as few as 22–23 observations captured every 16 d (in the case of CALIPSO). In order to validate the latter assumption in the context of a lidar mission, the following experiment was performed.

For each year, mean annual CA and CTH were calculated at 1, 2.5, 5 and 10° using the CALIPSO ground track for its 16 d revisit schedule. First, statistics were calculated for a revisit pattern that agreed with real-time mission overpasses (using the actual launch date of the satellite). Next, the same procedure was repeated 15 times, while in each iteration the pass date was incremented by one to replicate the situation where CALIPSO had been launched $1, 2, \ldots, 15$ d later than it actually was. Therefore, each location was characterized by 16 CA/CTH estimates, covering all possible launch dates. Finally, the highest and lowest values were examined. If the tested assumption was true, the difference between maximum and minimum values should be close to zero.

Table 3 shows the results of the simulation at sample locations. For instance, a 1° grid box centred at 16.5° N, 22.5° E reported maximum CA of 19.2 %, and a minimum of 9.6 %. Since CA for the actual pass day is known (9.6 %) it can be concluded that the mission coincided with the lowest of all 16 estimates. If the CALIPSO mission had been launched a few days later, the reported value would have been 19.2 %. It is important to note that although both values (as for any min–max range) are equally valid, only one was reported in the CALIPSO climatology – and then used in numerous applications.

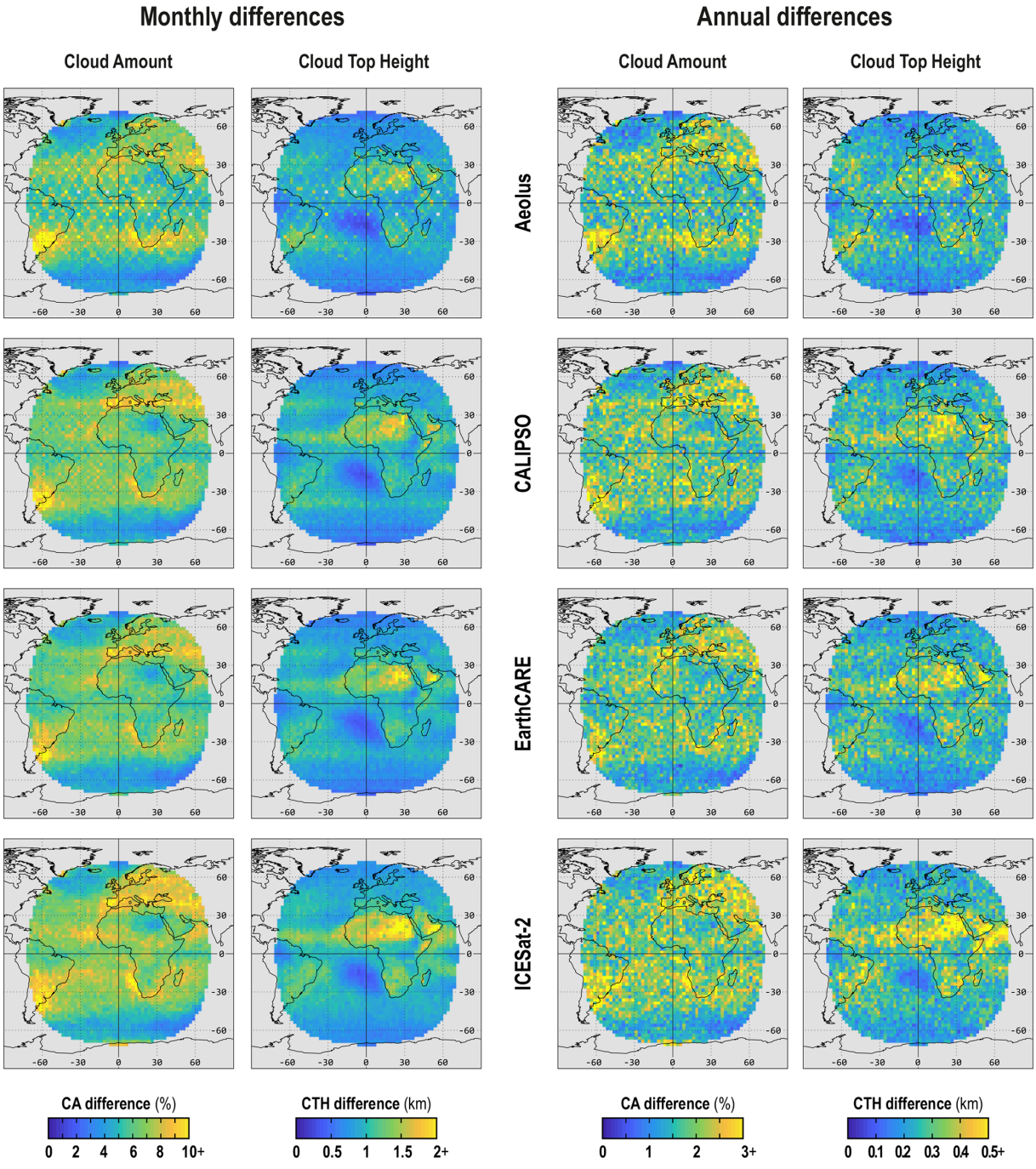

Figure 2. The geographical distribution of mean absolute differences between n day and 1 d revisit cloud amounts, and cloud top heights at monthly mean (left panel), and annual mean (right panel) timescales. In all cases, n day values are subtracted from 1 d values. Maps refer to 2.5° data.

For a grid box centred at 41.5° N, 31.5° E the spread of possible CA values in 2006 ranged from 41.4 % to 65.5 %, and the annual mean reported for the actual pass date (54.8 %) was in the middle of the range. However, in subsequent years, the value for the actual pass date matched the highest (2012), or the lowest (2007) estimate out of the 16 possible scenarios. It is only when CALIPSO transects are averaged into a 10 year annual mean that the value for the actual pass date will be in the middle of the min–max range, essentially being the value estimated for a 1 d revisit.

The results of the simulation for all locations and all spatial resolutions are shown in Fig. 5. Annual geographical distributions of differences between maximum and minimum CA/CTH duplicate the pattern reported for discrepancies be-

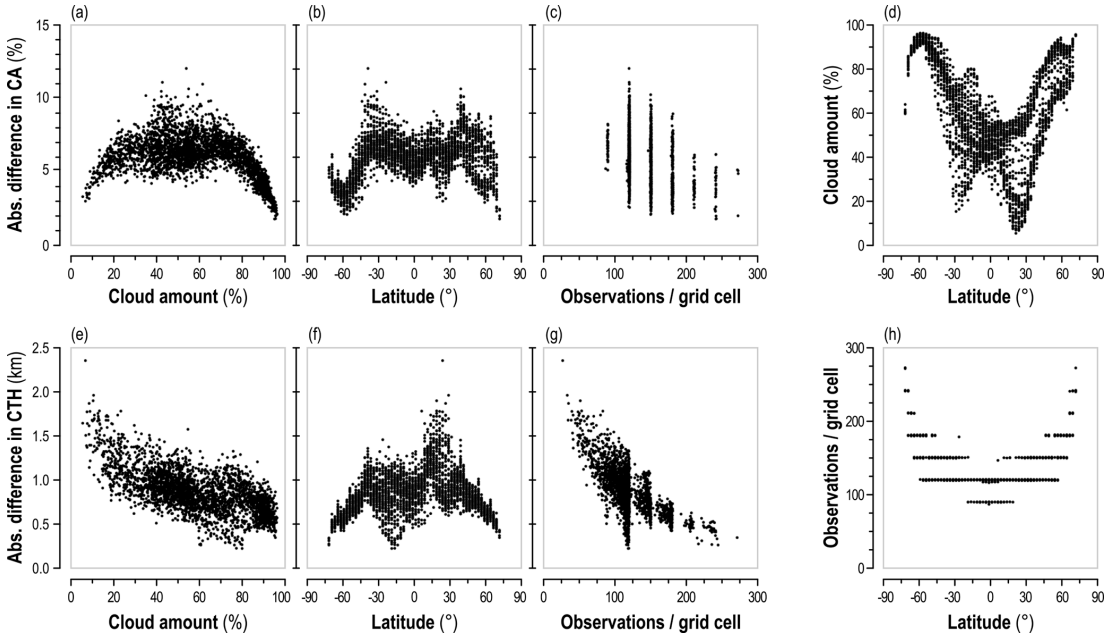

Figure 3. The relation between the mean annual difference in cloud amount **(a–c)**, and cloud top height **(e–g)** between *n* day and 1 d revisit climatologies, and: mean cloud amount **(a, e)**, latitude **(b, f)**, and the number of observations in the 1 d revisit scenario **(c, g)**. For reference, cloud amount in relation to latitude **(d)**, and the number of observations **(h)** is shown. Data refer to the simulated 2.5° resolution CALIPSO dataset.

Table 3. Cloud amount (%) for simulated CALIPSO-like scenarios, calculated for a single year and different locations (top rows), and multiple years at a single location (bottom rows). The table refers to results obtained at 1° spatial resolution. See text for details.

Grid box location; year	actual day	16 d revisit range for all possible days	location within range (%)	1 d revisit
		Single year, many locations		
16.5° N, 22.5° E; 2006	9.6	9.6–19.2	0	14.6
63.5° N, 20.5° E; 2006	76.3	58.1–76.3	100.0	68.5
35.1° N, 53.5° E; 2006	87.6	82.4–97.3	53.5	88.7
41.5° N, 31.5° E; 2006	54.8	41.4–65.5	55.5	55.0
		Single locations, various years		
41.5° N, 31.5° E; 2006	54.8	41.4–65.5	55.5	55.0
41.5° N, 31.5° E; 2007	42.8	42.8–56.8	0.0	49.3
41.5° N, 31.5° E; 2008	43.5	37.2–54.4	36.8	47.5
41.5° N, 31.5° E; 2009	53.7	41.4–64.9	52.4	51.1
41.5° N, 31.5° E; 2010	54.1	47.9–62.0	43.8	55.8
41.5° N, 31.5° E; 2011	59.8	37.2–60.5	97.1	52.6
41.5° N, 31.5° E; 2012	60.8	38.6–60.8	100.0	49.9
41.5° N, 31.5° E; 2013	42.7	39.0–67.4	13.2	51.7
41.5° N, 31.5° E; 2014	61.2	46.4–68.3	67.8	55.0
41.5° N, 31.5° E; 2015	44.8	34.7–68.0	30.3	53.2

tween 1 d and *n* day climatologies (Fig. 5c and d). Similarly, the width of the min-max range is a function of the spatial resolution of the target grid. For CA, it was typically over 14 % at 1°, and gradually narrowed to 7 % at 2.5°, and 3 % at 10° resolution (Fig. 5a). The corresponding change in CTH was from 1920 m (1°) to 1030 m (2.5°), and 370 m (at 10°) (Fig. 5b).

A dedicated indicator was introduced to map the coincidence between CA/CTH values on actual CALIPSO pass dates, and the max/min value of a parameter for all 16 in-

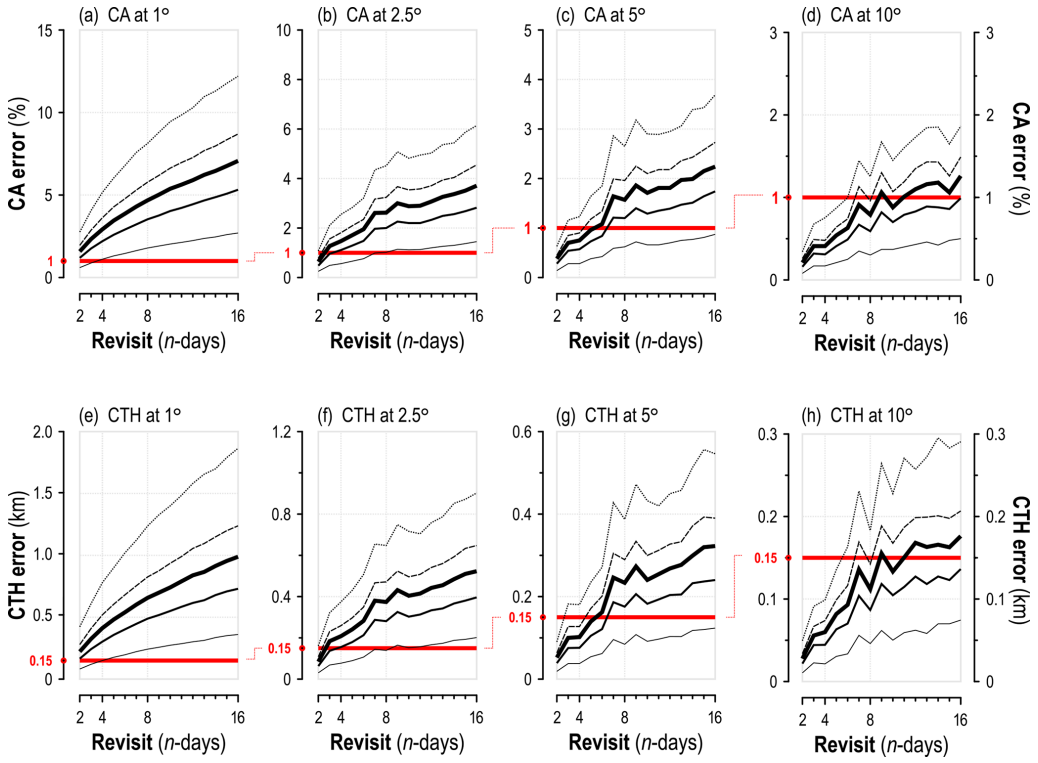

Figure 4. The spread of differences in cloud amount **(a–d)** and cloud top height **(e–h)** between 1 d and *n* day revisit climatologies, with respect to n ranging from 1–16 d. Data refer to the simulated 2.5° resolution CALIPSO dataset. Starting from the top-most, the lines indicate range covering: 99 % of observations (dotted line), 95 % (dashed line), 90 % (bold solid line), 80 % (regular solid line), and 50 % (thin solid line). Red bar indicated location of the accuracy threshold (see text for details). 16 d revisit can be achieved with one CALIPSO-like satellite, 8 d with two, 4 d with four, and 2 d with eight (phased orbits assumed). Note that for clarity the vertical scale has been adjusted for each plot.

vestigated scenarios. The min-max range was scaled to 0 %–100 %, and the CA/CTH value for the actual pass date was expressed on that scale. For example, 0 % meant that an estimate matched the lowest possible value, 100 % indicated that it matched the highest possible value, and at 50 % it agreed with the middle of the range.

The geographical distribution of the indicator was random for both CA (Fig. 5g) and CTH (Fig. 5h), thus two adjacent grid boxes could represent dramatically different tendencies. For a single year, it was unlikely that the annual mean would coincide with the middle of min-max range: only a quarter of locations reported a value between 40 % and 60 % (Fig. 5e and f). For up to ∼ 12 % of locations the CA/CTH value for the actual CALIPSO pass date represented the most extreme case (maximum and minimum CA/CTH values were matched in 16 scenarios). The randomness of the geographical distribution of the indicator, along with the statistical distribution of its value, had no relation to the spatial resolution of a grid.

4 Discussion

If we assume that a daily revisit regime represents true mean CA/CTH, the results of this study allow us to investigate the accuracy of lidar-based cloud climatologies used in climate change applications. Ohring et al. (2005) set two goals for satellite instrument calibration: 1 % for total CA, and 150 m for CTH. The latter values correspond well with upper accuracy thresholds set by the Global Climate Observing System for satellite-based data products (World Meteorological Organization, 2011).

Our study revealed that 1 % (CA) and 150 m (CTH) thresholds are beyond the capability of all investigated lidar missions, either at monthly or annual timescales (Table 4). As few as ∼ 5 %–15 % of locations (grid boxes) in the Meteosat domain met the 1 % criterion for CA and 150 m for CTH at the monthly scale, and at 1–2.5° spatial resolution. When gridded at a coarser resolution of 10°, roughly one third of grid boxes met CA/CTH accuracy criteria. Only when annual mean CA/CTH was considered did the majority (∼ 60 %) of grid boxes meet the requirements at (low) 5° spatial resolution.

Importantly, our study (see Table 2) only considered single-year monthly and annual means. On the other hand,

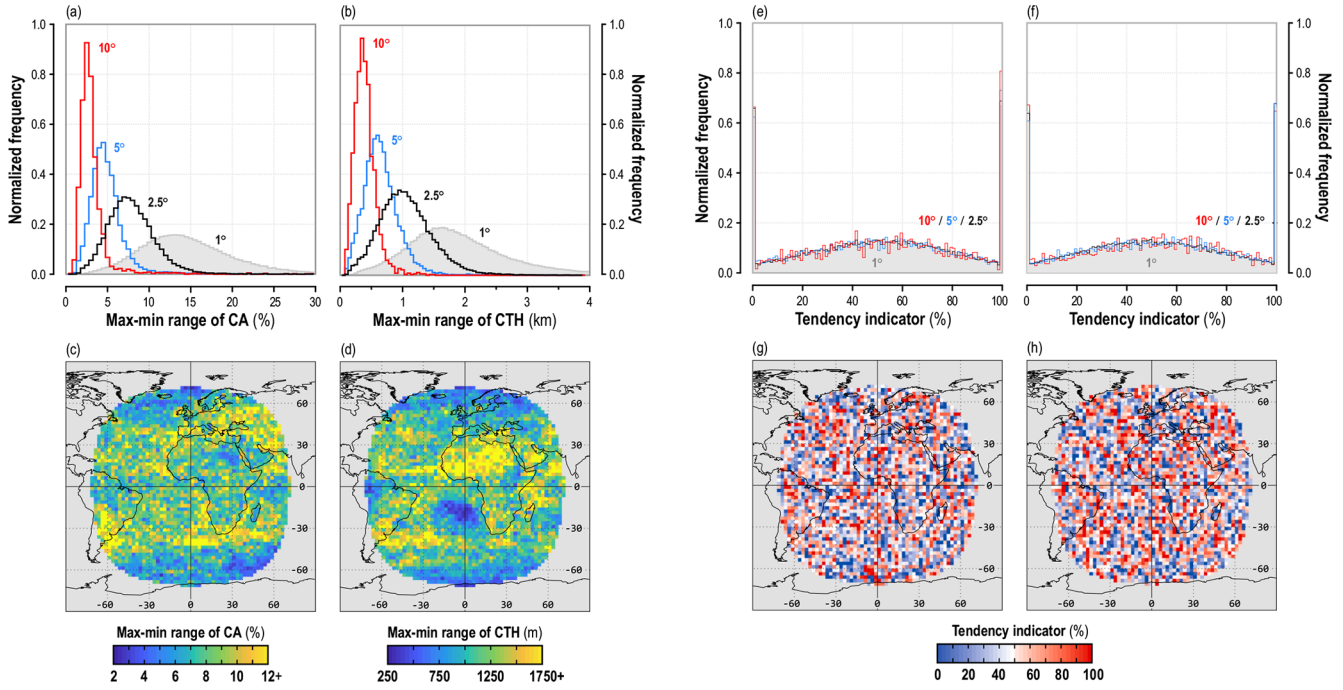

Figure 5. The range between maximum and minimum estimates of mean annual cloud amount **(c)**, and mean annual cloud top height **(d)** for all of the possible start dates for the CALIPSO ground track. The tendency for a parameter in the CALIPSO dataset from the actual launch date to be over- or underestimated is shown in **(g)** for cloud amount, and **(h)** for cloud top height. Maps **(c)**, **(d)**, **(g)**, and **(h)** only refer to the simulated 2.5° resolution CALIPSO dataset for 2008. Plots **(a)**, **(b)**, **(e)**, and **(f)** cover all resolutions considered.

the CALIPSO mission has provided ∼ 15 years of data. Table 4 suggests that when up to 10 years of observations are aggregated, it is realistic to expect 1 % accuracy in mean annual CA. However, this does not apply to the 10 year monthly mean: here, the total number of observations is comparable to the single-year annual mean, and therefore the magnitude of uncertainty will be similar to this mean.

One possible method to reduce errors is to increase the number of observations per year or month by increasing the number of satellites. However, as our CALIPSO-oriented experiment showed, the strategy will not be efficient in most cases. A 1 % (CA) or 150 m (CTH) accuracy for all 1 or 2.5° grid boxes would still require a daily revisit, meaning as many as 16 CALIPSO-like missions. Such a constellation is unlikely given the current CALIPSO technology and costs. However, the ongoing revolution in satellite technology (Stephens et al., 2020) and data processing (Yorks et al., 2021) may result in cost-effective small missions in the near future (e.g. the Time-varying Optical Measurements of Clouds and Aerosol Transport satellite, or the Methane Remote Sensing Lidar Mission; Ehret et al., 2017).

The second important finding reported here is that all lidar missions differed from the 1 d climatology in almost the same way (Figs. 1 and 2), despite their revisit frequency – however, only when the spatial resolution of the target grid was close to 5° or less. This means that at lower spatial resolution (larger grid box), an infrequent revisit schedule is compensated for by a denser ground track, and the effective number of observations is similar for all missions.

Our findings do not imply that CA and CTH from all missions will be exactly the same in real life. Lidar sensors onboard satellites differ in terms of both construction and their cloud detection algorithms. Furthermore, different satellites operate in orbits with different equatorial crossing times, therefore, CA/CTH values refer to different moments of the diurnal cycle (Noel et al., 2018).

In this context, CALIPSO and EarthCARE may be important exceptions. When launched, EarthCARE will be placed in an orbit with an equatorial crossing time at 14:00 LST, only 30 min after CALIPSO. Although the two missions will differ in terms of their equipment, the scientific community is seeking to standardize cloud detection algorithms, and make the final products coherent (Okamoto and Sato, 2018). If these efforts are successful, the only significant difference between the two missions will be their revisit frequency: 16 d for CALIPSO, and 25 d for EarthCARE. As this study has shown, this factor alone is not sufficient to result in significant differences. On the contrary, the two missions should provide almost the same CA/CTH statistics, and the EarthCARE mission's cloud climatology should be consistent with CALIPSO.

Finally, our study – for the very first time – has evaluated the magnitude of possible uncertainties resulting from the infrequent sampling regime of lidar missions, based on realistic

Table 4. The fraction (%) of locations (specifically, grid boxes within the Meteosat field of view) that met the accuracy criterion of 1 % for cloud amount (CA), and 150 m for cloud top height (CTH), at monthly and annual timescales.

Lidar	Monthly		Annual	
mission	CA	CTH	CA	CTH
	$1 \times 1^\circ$ grid box size			
Aeolus	9	10	27	31
CALIPSO	6	7	20	23
EarthCARE	6	7	20	22
ICESat	6	6	19	21
	$2.5 \times 2.5^\circ$ grid box size			
Aeolus	12	14	39	42
CALIPSO	12	13	37	40
EarthCARE	12	13	37	40
ICESat	11	12	35	37
	$5 \times 5^\circ$ grid box size			
Aeolus	19	21	58	61
CALIPSO	19	20	56	59
EarthCARE	20	21	59	60
ICESat	19	20	57	59
	$10 \times 10^\circ$ grid box size			
Aeolus	33	36	84	85
CALIPSO	32	34	83	84
EarthCARE	34	35	86	87
ICESat	31	31	82	82

cloud data (empirical cloud regimes, and how they are distributed geographically). Our results suggest that some practical considerations should be taken into account when using lidar data to validate other cloud climatologies or models.

According to Winker et al. (2017), nadir-only observations should (theoretically) provide sufficient sampling accuracy at monthly and annual global scales. Specifically, root mean square error for CA should be < 1 % (Ohring et al., 2005). The present study confirmed that this thesis is valid for all investigated lidars, and also demonstrated that 1 % accuracy can be achieved for ~ 80 % of locations at $10 \times 10^\circ$, assuming 1 d revisit data as true CA (Table 4). However, at the finer resolutions typically used to investigate the geographical distribution of CA/CTH (1–2.5°), accuracies were much lower, and failed to meet required standards.

Our CALIPSO-focused experiments (Sect. 3.3) demonstrated that the single-year annual mean (at grid box level) is very sensitive even to theoretically irrelevant aspects such as the initial day of the revisit cycle. Shifting this date backward or forward by one day may result in a significantly different estimate of mean annual CA, and this finding must be taken into account when CALIPSO data are used for validation. For instance, Heidinger et al. (2012) compared 2007 mean annual CA from the Advanced Very High Resolution Radiometer to CALIPSO estimates for the same year. Locally, differences between datasets were up to 10 %–20 %. However, the present study revealed that as much as 15 % of the difference in CA can be attributed to uncertainty related to CALIPSO's infrequent and sparse sampling regime. Similarly, Franklin et al. (2013) used mean seasonal CA from CALIPSO as validation data, but neglected uncertainty in lidar estimates at such a short timescale. Finally, Chepfer et al. (2008) compared day and night CA from CALIPSO using 3 month means. Although discrepancies reached ± 25 %, the authors did not discuss the impact of infrequent sampling.

The experiment described in Sect. 3.3 only considered uncertainties that resulted from the shift of the initial day of the cycle. Other sources of uncertainty have been ignored. Similarly, Sect. 3.1 only compared differences between n day and 1 d climatologies, ignoring other aspects. In this way, individual sources of uncertainty in CA/CTH estimation were investigated. The results showed that shifting the initial day of the revisit cycle can lead to higher uncertainty than sampling every n days. For instance, globally and at 2.5° the average range in CA uncertainty due to the shift of the initial day of the cycle was 7% (i.e. mean ± 3.5 %), while the standard deviation of differences between n day and 1 d estimates was 2.2 %. With this configuration, the magnitude of uncertainty is of the same order, but – as the study showed – local, per grid cell differences may be higher. Consequently, at fine spatial resolution, the uncertainty budget has to be calculated individually to test how uncertainties from different sources interfere.

Sparse sampling and an infrequent revisit schedule have most impact on short-term, lidar-based cloud climatologies. Therefore, whenever a single-year annual mean is validated, the resulting lidar climatology should not be considered as a point estimate (mean value), but rather as a confidence interval for the mean (e.g. Kotarba and Solecki, 2021). An alternative approach is to match individual lidar profiles with imagers on a per-pixel basis (Wang et al., 2016; Kotarba 2020; Heidinger et al., 2012). Unfortunately, this is only possible in the rare cases where the lidar's and imager's orbits are aligned.

Addressing uncertainties in CA and CTH, as found in this study, is also important for calculating radiative effects related to clouds. Differences between n day and 1 d climatologies showed that at the local scale (grid cell level) monthly uncertainties due to sampling frequency can exceed 10 % at each spatial resolution (although more frequently at a finer level of detail; Fig. 1). Under- or over-estimation in CA by ~ 10 %, or 2–3 km in CTH, may change radiative transfer results dramatically. Consequently, single-year monthly cloud radiative effects estimated locally with lidar-based cloud data should be interpreted with the highest degree of caution. The suggested approach would be to use uncertainty ranges of CA/CTH, as reported in this study (or derived individually

for a given study), to find upper and lower bounds of the uncertainty range for the cloud radiative property under study.

More research is needed to test how the lidar's revisit schedule should be accounted for in satellite simulators (e.g. the CFMIP Observation Simulator Package, COSP; Bodas-Salcedo et al., 2011). The goal of simulators is to reduce bias between satellite-observed and model-generated cloud parameters. This is achieved by producing satellite-like radiances from a modelled atmosphere, then retrieving sensor-specific data for the desired geophysical variable. Unfortunately, satellite sampling factors (the revisit frequency, the ground track density) are typically neglected in satellite simulators. Consequently, simulated lidar-like cloud parameters resemble a daily revisit mission, rather than actual n day sampling. This source of bias remains largely unaddressed. On the other hand, model validations tend to use long time series (10+ years) of CALIPSO observations, which greatly increases the number of observations that shape the annual mean. As a consequence, revisit-related uncertainties become relatively limited.

5 Summary and Conclusion

This study is the first of its kind to compare lidar cloud climatologies (CA, CTH) for a hypothetical 1 d revisit, and the actual n day revisit regime (where n is mission specific). We considered four missions: CALIPSO ($n = 16$), EarthCARE ($n = 25$), Aeolus ($n = 7$), and ICESat-2 ($n = 91$), with a special focus on CALIPSO, as it has contributed most to cloud climatology studies. Statistics for 10 years of observations (2007–2016) were evaluated, taking into account both spatial (ground track density), and temporal (the actual temporal sequence of the orbit during the revisit cycle) sampling scenarios. Highly-reliable, Meteosat 15 min data were used as the source of real CA and CTH, and to understand how the two parameters actually vary in time and space (realistic cloud regimes).

Our central hypothesis was that cloud parameters estimated from an n day revisit mission do not differ significantly from values that would be obtained with a daily revisit schedule. The results of our simulation demonstrate that this hypothesis is invalid for most of the evaluated circumstances. Specifically:

- assuming a 1 d revisit regime as a proxy for true CA/CTH, the actual (n day) revisit schedule was insufficient to calculate mean annual values of parameters that met required accuracies (1 % for CA, 150 m for CTH), at a spatial resolution better than 10° latitude and longitude. This required accuracy was only achieved at the mean global scale, and only for most ($\sim 80\,\%$) $10 \times 10°$ grid boxes;

- mean annual CA is very sensitive to the revisit frequency, and the corresponding ground track density. For a single year, revisit-related uncertainties for CA/CTH can be as high as 15 % per 1800 m (on average) when lidar transects are gridded at 1° resolution, or 5 % per 1000 m when gridded at 2.5° resolution. As a consequence, whenever lidar data are used to validate other cloud datasets (either empirical or modelled), the revisit time should be accounted for by using, for example, confidence intervals instead of point estimates (mean, median). Confidence intervals provide information about uncertainty related to a statistic, which is not achievable with a point estimate alone. Depending on the distribution of the variable, intervals can be calculated using mean and standard deviation (when the variable follows a normal distribution) or with, for example, the bootstrap approach (where no assumptions about the distribution are required; DiCiccio and Efron, 1996);

- despite their different revisit frequencies, we found a similar magnitude of discrepancy for all of the investigated lidars (CALIPSO, Aeolus, ICESat-2, EarthCARE), between the hypothetical 1 d revisit mission, and the actual n day revisit climatology – especially at lower resolutions ($\leq 2.5°$). The latter finding suggests that at this scale of aggregation, infrequent revisits are compensated for by the ground track density. It also suggests that CALIPSO, together with its follow-on mission EarthCARE, are very likely to produce consistent cloud records despite the difference in sampling frequency.

The present study implemented a simulation method that can test uncertainties in individual lidar missions, or tandem polar-orbiting + inclined-orbit lidar constellations (CALIPSO–CATS, or the AOS-P1–AOS-I1 concept that has been studied under NASA's Atmosphere Observing System, http://aos.gsfc.nasa.gov/, last access: 21 June 2022). When a single lidar mission is considered, the method can also be used globally with a polar-orbiting imager that shares the same revisit frequency and equatorial crossing time (currently this is only possible for CALIPSO, simulated with MODIS/Aqua). If this is not possible, any geostationary platform or high-frequency atmospheric model can be used instead.

Data availability. Data analysed in this study were a re-analysis of METEOSAT cloud data, that are openly available from the EUMETSAT Satellite Application Facility on Climate Monitoring (CM SAF; https://doi.org/10.5676/EUM_SAF_CM/CLAAS/V002_01, Finkensieper et al., 2020).

Competing interests. The author has declared that there are no competing interests.

Financial support. This research has been supported by the National Science Centre of Poland (grant no. UMO-2017/25/B/ST10/01787) and the Infrastruktura PL-Grid (grant no. plgmodis4).

Review statement. This paper was edited by Andrew Sayer and reviewed by David Winker and J. Yorks.

References

Ackerman, S. A., Holz, R. E., Frey, R., Eloranta, E. W., Maddux, B. C., and McGill, M.: Cloud detection with MODIS. Part II: Validation, J. Atmos. Ocean. Technol., 25, 1073–1086, https://doi.org/10.1175/2007JTECHA1053.1, 2008.

Adhikari, L., Wang, Z., and Deng, M.: Seasonal variations of Antarctic clouds observed by CloudSat and CALIPSO satellites, J. Geophys. Res.-Atmos., 117, D04202, https://doi.org/10.1029/2011JD016719, 2012.

Benas, N., Finkensieper, S., Stengel, M., van Zadelhoff, G.-J., Hanschmann, T., Hollmann, R., and Meirink, J. F.: The MSG-SEVIRI-based cloud property data record CLAAS-2, Earth Syst. Sci. Data, 9, 415–434, https://doi.org/10.5194/essd-9-415-2017, 2017.

Bodas-Salcedo, A., Webb, M. J., Bony, S., Chepfer, H., Dufresne, J.-L., Klein, S. A., Zhang, Y., Marchand, R., Haynes, J. M., Pincus, R., and John, V. O.: COSP: Satellite simulation software for model assessment, Bull. Am. Meteorol. Soc., 92, 1023–1043, https://doi.org/10.1175/2011BAMS2856.1, 2011.

Boudala, F. S. and Milbrandt, J. A.: Evaluations of the Climatologies of Three Latest Cloud Satellite Products Based on Passive Sensors (ISCCP-H, Two CERES) against the CALIPSO-GOCCP, Remote Sens., 13, 5150, https://doi.org/10.3390/rs13245150, 2021.

Braun, B. M., Sweetser, T. H., Graham, C., and Bartsch, J.: CloudSat's A-Train Exit and the Formation of the C-Train: An Orbital Dynamics Perspective, in: IEEE Aerosp. Conf. Proc., Big Sky, Montana, USA, 2–9 March 2019, CFP19AAC-POD, 4708–4717, ISBN 978-1-5386-6855-9, 2019.

Capderou, M.: Motion of Orbit, Earth and Sun, in: Satellites: Orbits and Missions, Springer, Paris, 129–173, ISBN 978-2287213175, 2005.

Chepfer, H., Bony, S., Winker, D., Chiriaco, M., Dufresne, J.-L., and Sèze, G.: Use of CALIPSO lidar observations to evaluate the cloudiness simulated by a climate model, Geophys. Res. Lett., 35, L15704, https://doi.org/10.1029/2008GL034207, 2008.

Chepfer, H., Bony, S., Winker, D., Cesana, G., Dufresne, J. L., Minnis, P., Stubenrauch, C. J., and Zeng, S.: The GCM-oriented CALIPSO cloud product (CALIPSO-GOCCP), J. Geophys. Res.-Atmos., 115, D00H16, https://doi.org/10.1029/2009JD012251, 2010.

Daisuke, S., Trung, N. T., Rei, M., Yoshito, S., Tadashi, I., and Toshiyoshi, K.: Progress of the ISS Based Vegetation LiDAR Mission, Moli – Japan's First Space-Based LiDAR, in: IGARSS 2020, 2020 IEEE Int. Geosci. Remote Se., virtual, 26 September–2 October 2020, 3467–3470, https://doi.org/10.1109/IGARSS39084.2020.9323332, 2020.

DiCiccio, T. J. and Efron, B.: Bootstrap confidence intervals, Stat. Sci., 11, 189–228, https://doi.org/10.1214/ss/1032280214, 1996.

Ehret, G., Bousquet, P., Pierangelo, C., Alpers, M., Millet, B., Abshire, J. B., Bovensmann, H., Burrows, J. P., Chevallier, F., Ciais, P., Crevoisier, C., Fix, A., Flamant, P., Frankenberg, C., Gibert, F., Heim, B., Heimann, M., Houweling, S., Hubberten, H. W., Jöckel, P., Law, K., Löw, A., Marshall, J., Agusti-Panareda, A., Payan, S., Prigent, C., Rairoux, P., Sachs, T., Scholze, M., and Wirth, M.: MERLIN: A French-German Space Lidar Mission Dedicated to Atmospheric Methane, Remote Sens., 9, 1052, https://doi.org/10.3390/rs9101052, 2017.

Finkensieper, S., Meirink, J.-F., van Zadelhoff, G.-J., Hanschmann, T., Benas, N., Stengel, M., Fuchs, P., Hollmann, R., Kaiser, J., and Werscheck, M.: CLAAS-2.1: CM SAF CLoud property dAtAset using SEVIRI – Edition 2.1, Satellite Application Facility on Climate Monitoring [data set], https://doi.org/10.5676/EUM_SAF_CM/CLAAS/V002_01, 2020.

Flamant, P., Cuesta, J., Denneulin, M.-L., Dabas, A., and Huber, D.: ADM-Aeolus retrieval algorithms for aerosol and cloud products, Tellus A Dyn. Meteorol. Oceanogr., 60, 273–286, https://doi.org/10.1111/j.1600-0870.2007.00287.x, 2008.

Franklin, C. N., Sun, Z., Bi, D., Dix, M., Yan, H., and Bodas-Salcedo, A.: Evaluation of clouds in ACCESS using the satellite simulator package COSP: Global, seasonal, and regional cloud properties, J. Geophys. Res.-Atmos., 118, 732–748, https://doi.org/10.1029/2012JD018469, 2013.

Heidinger, A. K., Evan, A. T., Foster, M. J., and Walther, A.: A naive Bayesian cloud-detection scheme derived from Calipso and applied within PATMOS-x, J. Appl. Meteorol. Climatol., 51, 1129–1144, https://doi.org/10.1175/JAMC-D-11-02.1, 2012.

Holz, R. E., Ackerman, S. A., Nagle, F. W., Frey, R., Dutcher, S., Kuehn, R. E., Vaughan, M. A., and Baum, B.: Global Moderate Resolution Imaging Spectroradiometer (MODIS) cloud detection and height evaluation using CALIOP, J. Geophys. Res.-Atmos., 114, D00A19, https://doi.org/10.1029/2008JD009837, 2009.

Hunt, W. H., Vaughan, M. A., Powell, K. A., and Weimer, C.: CALIPSO lidar description and performance assessment, J. Atmos. Ocean. Technol., 26, 1214–1228, https://doi.org/10.1175/2009JTECHA1223.1, 2009.

Illingworth, A. J., Barker, H. W., Beljaars, A., Ceccaldi, M., Chepfer, H., Clerbaux, N., Cole, J., Delanoë, J., Domenech, C., Donovan, D. P., Fukuda, S., Hirakata, M., Hogan, R. J., Huenerbein, A., Kollias, P., Kubota, T., Nakajima, T., Nakajima, T. Y., Nishizawa, T., Ohno, Y., Okamoto, H., Oki, R., Sato, K., Satoh, M., Shephard, M. W., Velázquez-Blázquez, A., Wandinger, U., Wehr, T., and Van Zadelhoff, G. J.: The earthcare satellite: The next step forward in global measurements of clouds, aerosols, precipitation, and radiation, Bull. Am. Meteorol. Soc., 96, 1311–1332, https://doi.org/10.1175/BAMS-D-12-00227.1, 2015.

Kodama, C., Noda, A. T., and Satoh, M.: An assessment of the cloud signals simulated by NICAM using ISCCP, CALIPSO, and CloudSat satellite simulators, J. Geophys. Res.-Atmos., 117, D12210, https://doi.org/10.1029/2011JD017317, 2012.

Konsta, D., Dufresne, J.-L., Chepfer, H., Idelkadi, A., and Cesana, G.: Use of A-train satellite observations (CALIPSO–PARASOL) to evaluate tropical cloud properties in the LMDZ5 GCM, Clim. Dyn., 47, 1263–1284, https://doi.org/10.1007/s00382-015-2900-y, 2016.

Kotarba, A. Z.: Calibration of global MODIS cloud amount using CALIOP cloud profiles, Atmos. Meas. Tech., 13, 4995–5012, https://doi.org/10.5194/amt-13-4995-2020, 2020.

Kotarba, A. Z. and Solecki, M.: Uncertainty Assessment of the Vertically-Resolved Cloud Amount for Joint CloudSat–CALIPSO Radar–Lidar Observations, Remote Sens., 13, 807, https://doi.org/10.3390/rs13040807, 2021.

Liu, Y., Ackerman, S. A., Maddux, B. C., Key, J. R., and Frey, R. A.: Errors in cloud detection over the arctic using a satellite imager and implications for observing feedback mechanisms, J. Clim., 23, 1894–1907, https://doi.org/10.1175/2009JCLI3386.1, 2010.

Liu, Y., Key, J. R., Ackerman, S. A., Mace, G. G., and Zhang, Q.: Arctic cloud macrophysical characteristics from CloudSat and CALIPSO, Remote Sens. Environ., 124, 159–173, https://doi.org/10.1016/j.rse.2012.05.006, 2012.

Liu, Z., Vaughan, M., Winker, D., Kittaka, C., Getzewich, B., Kuehn, R., Omar, A., Powell, K., Trepte, C., and Hostetler, C.: The CALIPSO lidar cloud and aerosol discrimination: Version 2 algorithm and initial assessment of performance, J. Atmos. Ocean. Technol., https://doi.org/10.1175/2009JTECHA1229.1, 2009.

Ma, X., Bartlett, K., Harmon, K., and Yu, F.: Comparison of AOD between CALIPSO and MODIS: significant differences over major dust and biomass burning regions, Atmos. Meas. Tech., 6, 2391–2401, https://doi.org/10.5194/amt-6-2391-2013, 2013.

Mace, G. G. and Zhang, Q.: The CloudSat radar-lidar geometrical profile product (RL-GeoProf): Updates, improvements, and selected results, J. Geophys. Res., 119, 9441–9462, https://doi.org/10.1002/2013JD021374, 2014.

Mace, G. G., Zhang, Q., Vaughan, M., Marchand, R., Stephens, G., Trepte, C., and Winker, D.: A description of hydrometeor layer occurrence statistics derived from the first year of merged Cloudsat and CALIPSO data, J. Geophys. Res.-Atmos., 114, D00A26, https://doi.org/10.1029/2007JD009755, 2009.

Markus, T., Neumann, T., Martino, A., Abdalati, W., Brunt, K., Csatho, B., Farrell, S., Fricker, H., Gardner, A., Harding, D., Jasinski, M., Kwok, R., Magruder, L., Lubin, D., Luthcke, S., Morison, J., Nelson, R., Neuenschwander, A., Palm, S., Popescu, S., Shum, C. K., Schutz, B. E., Smith, B., Yang, Y., and Zwally, J.: The Ice, Cloud, and land Elevation Satellite-2 (ICESat-2): Science requirements, concept, and implementation, Remote Sens. Environ., 190, 260–273, https://doi.org/10.1016/j.rse.2016.12.029, 2017.

Nazaryan, H., McCormick, M. P., and Menzel, W. P.: Global characterization of cirrus clouds using CALIPSO data, J. Geophys. Res.-Atmos., 113, D16211, https://doi.org/10.1029/2007JD009481, 2008.

Noel, V., Chepfer, H., Chiriaco, M., and Yorks, J.: The diurnal cycle of cloud profiles over land and ocean between 51° S and 51° N, seen by the CATS spaceborne lidar from the International Space Station, Atmos. Chem. Phys., 18, 9457–9473, https://doi.org/10.5194/acp-18-9457-2018, 2018.

Ohring, G., Wielicki, B., Spencer, R., Emery, B., and Datla, R.: Satellite instrument calibration for measuring global climate change: Report of a workshop, Bull. Am. Meteorol. Soc., 86, 1303–1314, https://doi.org/10.1175/BAMS-86-9-1303, 2005.

Okamoto, H. and Sato, K.: Cloud Remote Sensing by Active Sensors: New Perspectives from CloudSat, CALIPSO and EarthCARE BT – Remote Sensing of Clouds and Precipitation, 1st edn., edited by: Andronache, C., Springer International Publishing, Cham, 195–214, https://doi.org/10.1007/978-3-319-72583-3, 2018.

Oreopoulos, L., Cho, N., and Lee, D.: New insights about cloud vertical structure from CloudSat and CALIPSO observations, J. Geophys. Res.-Atmos., 122, 9280–9300, https://doi.org/10.1002/2017JD026629, 2017.

Palm, S. P., Yang, Y., Herzfeld, U., Hancock, D., Hayes, A., Selmer, P., Hart, W., and Hlavka, D.: ICESat-2 Atmospheric Channel Description, Data Processing and First Results, Earth Sp. Sci., 8, e2020EA001470, https://doi.org/10.1029/2020EA001470, 2021.

Stengel, M., Kniffka, A., Meirink, J. F., Lockhoff, M., Tan, J., and Hollmann, R.: CLAAS: the CM SAF cloud property data set using SEVIRI, Atmos. Chem. Phys., 14, 4297–4311, https://doi.org/10.5194/acp-14-4297-2014, 2014.

Stephens, G., Freeman, A., Richard, E., Pilewskie, P., Larkin, P., Chew, C., Tanelli, S., Brown, S., Posselt, D., and Peral, E.: The Emerging Technological Revolution in Earth Observations, Bull. Am. Meteorol. Soc., 101, E274–E285, https://doi.org/10.1175/BAMS-D-19-0146.1, 2020.

Stephens, G. L.: Cloud Feedbacks in the Climate System: A Critical Review, J. Clim., 18, 237–273, https://doi.org/10.1175/JCLI-3243.1, 2005.

Stephens, G. L. and Kummerow, C. D.: The Remote Sensing of Clouds and Precipitation from Space: A Review, J. Atmos. Sci., 64, 3742–3765, https://doi.org/10.1175/2006JAS2375.1, 2007.

Stoffelen, A., Pailleux, J., Källén, E., Vaughan, J. M., Isaksen, L., Flamant, P., Wergen, W., Andersson, E., Schyberg, H., Culoma, A., Meynart, R., Endemann, M., and Ingmann, P.: The Atmospheric Dynamics Mission For Global Wind Field Measurement, Bull. Am. Meteorol. Soc., 86, 73–88, https://doi.org/10.1175/BAMS-86-1-73, 2005.

Tang, H., Armston, J., Hancock, S., Marselis, S., Goetz, S., and Dubayah, R.: Characterizing global forest canopy cover distribution using spaceborne lidar, Remote Sens. Environ., 231, 111262, https://doi.org/10.1016/j.rse.2019.111262, 2019.

Trenberth, K. E., Fasullo, J. T., and Kiehl, J.: Earth's global energy budget, Bull. Am. Meteorol. Soc., 90, 311–323, https://doi.org/10.1175/2008BAMS2634.1, 2009.

Vaughan, M. A., Powell, K. A., Kuehn, R. E., Young, S. A., Winker, D. M., Hostetler, C. A., Hunt, W. H., Liu, Z., Mcgill, M. J., and Getzewich, B. J.: Fully automated detection of cloud and aerosol layers in the CALIPSO lidar measurements, J. Atmos. Ocean. Technol., 26, 2034–2050, https://doi.org/10.1175/2009JTECHA1228.1, 2009.

Wang, T., Fetzer, E. J., Wong, S., Kahn, B. H., and Yue, Q.: Validation of MODIS cloud mask and multilayer flag using CloudSat-CALIPSO cloud profiles and a cross-reference of their cloud classifications, J. Geophys. Res.-Atmos., 121, 11620–11635, https://doi.org/10.1002/2016JD025239, 2016.

Winker, D., Chepfer, H., Noel, V., and Cai, X.: Observational Constraints on Cloud Feedbacks: The Role of Active Satellite Sensors, Surv. Geophys., 38, 1483–1508, https://doi.org/10.1007/s10712-017-9452-0, 2017.

Winker, D. M., Pelon, J. R., and McCormick, M. P.: The CALIPSO mission: spaceborne lidar for observation of aerosols and clouds, Lidar Remote Sens. Ind. Environ. Monit. III, 4893, 1, https://doi.org/10.1117/12.466539, 2003.

World Meteorological Organization: Systematic Observation Requirements for Satellite-based Products for Climate – Supplemental details to the satellite-based component of the "Implementation Plan for the Global Observing System for Climate in Support of the UNFCCC (2010 update)", GCOS – 154, https://library.wmo.int/doc_num.php?explnum_id=3710 (last access: 21 June 2022), 2011.

Wylie, D., Eloranta, E., Spinhirne, J. D., and Palm, S. P.: A comparison of cloud cover statistics from the GLAS lidar with HIRS, J. Clim., 20, 4968–4981, https://doi.org/10.1175/JCLI4269.1, 2007.

Yorks, J. E., McGill, M. J., Palm, S.P. , Hlavka, D. L. , Selmer, P.A. , Nowottnick, E. , Vaughan, M. A. , Rodier, S., and Hart W. D.: An Overview of the CATS Level 1 Data Products and Processing Algorithms, Geophys. Res. Lett., 43, 4632–4639, https://doi.org/10.1002/2016GL068006, 2016.

Yorks, J. E., Selmer, P. A., Kupchock, A., Nowottnick, E. P., Christian, K. E., Rusinek, D., Dacic, N., and McGill, M. J.: Aerosol and Cloud Detection Using Machine Learning Algorithms and Space-Based Lidar Data, Atmosphere, 12, 606, https://doi.org/10.3390/atmos12050606, 2021.